

Parton distributions: determining probabilities in a space of functions

The NNPDF Collaboration: *Richard D. Ball*¹, *Valerio Bertone*², *Francesco Cerutti*³,
*Luigi Del Debbio*¹, *Stefano Forte*⁴, *Alberto Guffanti*⁵, *José I. Latorre*³, *Juan Rojo*^{4*} and *Maria Ubiali*⁶.

¹ School of Physics and Astronomy, University of Edinburgh,
JCMB, KB, Mayfield Rd, Edinburgh EH9 3JZ, Scotland

² Physikalisches Institut, Albert-Ludwigs-Universität Freiburg,
Hermann-Herder-Straße 3, D-79104 Freiburg i. B., Germany

³ Departament d'Estructura i Constituents de la Matèria, Universitat de Barcelona,
Diagonal 647, E-08028 Barcelona, Spain

⁴ Dipartimento di Fisica, Università di Milano and INFN, Sezione di Milano,
Via Celoria 16, I-20133 Milano, Italy

⁵ The Niels Bohr International Academy and Discovery Center,
The Niels Bohr Institute, Blegdamsvej 17, DK-2100 Copenhagen, Denmark

⁶ Institut für Theoretische Teilchenphysik und Kosmologie, RWTH Aachen University,
D-52056 Aachen, Germany

Abstract

We discuss the statistical properties of parton distributions within the framework of the NNPDF methodology. We present various tests of statistical consistency, in particular that the distribution of results does not depend on the underlying parametrization and that it behaves according to Bayes' theorem upon the addition of new data. We then study the dependence of results on consistent or inconsistent datasets and present tools to assess the consistency of new data. Finally we estimate the relative size of the PDF uncertainty due to data uncertainties, and that due to the need to infer a functional form from a finite set of data.

1 The NNPDF approach to parton distributions

The determination of parton distributions (PDFs) and their uncertainties [1] poses a difficult problem because one is trying to determine the probability distribution for a set of functions. Given that this is necessarily done from a finite set of data it requires some assumptions: some of these, such as a certain degree of smoothness, may be physically motivated, but it is important to check that they do not bias the result and in particular that they do not destroy its statistical interpretation. The most common way of implementing these assumptions is to assume a functional form for the PDFs, each parametrized by a small number of parameters (typically between two and five) which are determined by fitting a suitable set of data. The NNPDF collaboration has developed an alternative approach [2–9] which tries to avoid the bias associated to this procedure.

The NNPDF approach is based on four main ingredients:

- *Monte Carlo by importance sampling.* NNPDF produces a Monte Carlo sampling of the probability density in the (function) space of PDFs. To adequately sample this space by simple binning would be simply impossible: for example assuming seven PDFs (the three light quarks and anti-quarks and the gluon) sampled at ten points, binning the probability distribution in each direction with five bins one would end up with $5^{70} \sim 10^{49}$ bins. The problem is solved by importance sampling: most bins are empty and only those with data are relevant. Hence, one starts by constructing a set of data replicas, which reproduces the statistical features of the original data. It then turns out

*Now at PH Department, TH Unit, CERN, CH-1211 Geneva 23, Switzerland

that a sample of 1000 pseudo-data replicas is large enough to reproduce central values, uncertainty and correlations of the starting data to a few percent accuracy

- *Neural networks as universal unbiased interpolants.* Each of the underlying functions is parametrized with a feed-forward multilayer neural network. The architecture chosen corresponds to 37 free parameters for each of the seven PDFs. It can then be checked that results do not depend on the parametrization by verifying that they are unchanged if the size of the neural network is reduced.
- *Genetic Algorithms for neural network training.* The best fit is determined by using a genetic algorithm, and starting from a random initialization of parameters. This ensures that the presumably wide space of equivalent minima can be adequately explored.
- *Determination of the best fit by cross-validation.* Because the parametrization is very large, the best fit is not the minimum of the χ^2 , which would correspond to fitting noise. The best fit is then found by dividing randomly data in two sets (training and validation) for each experiment, minimizing the χ^2 of the training set while monitoring the χ^2 of both sets. The best-fit is obtained when the χ^2 of the validation set starts increasing despite the fact that the χ^2 of the training set still decreases.

2 Statistical consistency

Our starting point is the NNPDF2.1 NLO [9] PDF set: we would like to test that it behaves in a statistically consistent way. For a start, in Table 1 we show the statistical estimators for this PDF fit: χ_{tot}^2 is the result of the comparison to data of the best-fit PDFs (defined as the average over the $N_{\text{rep}} = 1000$ replicas of the Monte Carlo sample); $\langle \chi^{2(k)} \rangle$ is the average of the values obtained by comparing each PDF replica to the data, and $\langle E \rangle$ is the value of the same figure of merit, but obtained comparing each PDF replica to the corresponding data replica. For the latter, the training and validation values are also shown. All figures of merit are computed using the full covariance matrix, with normalization uncertainties included using the so-called t_0 method of Ref. [10]; they are all normalized to the number of data points N_{dat} . The fact that $\langle \chi^{2(k)} \rangle \sim 1$ while $\langle E \rangle \sim 2$, and also that $\chi_{\text{tot}}^2 < \langle \chi^{2(k)} \rangle$ are both consistent with the fact that the fit is “learning” an underlying law: the fitted PDFs are closer to the data than the data replicas (despite being fitted to the latter), and the best fit (obtained averaging replicas) is yet closer to the data than any of the individual replicas.

| | Reference | Central Values | Average Fixed Partitions |
|--|-----------------|-----------------|--------------------------|
| χ_{tot}^2 | 1.16 | 1.14 | 1.15 |
| $\langle E \rangle \pm \sigma_E$ | 2.24 ± 0.09 | 1.25 ± 0.11 | 1.24 ± 0.07 |
| $\langle E_{\text{tr}} \rangle \pm \sigma_{E_{\text{tr}}}$ | 2.22 ± 0.11 | 1.25 ± 0.12 | 1.23 ± 0.07 |
| $\langle E_{\text{val}} \rangle \pm \sigma_{E_{\text{val}}}$ | 2.28 ± 0.12 | 1.27 ± 0.11 | 1.26 ± 0.08 |
| $\langle \chi^{2(k)} \rangle \pm \sigma_{\chi^2}$ | 1.25 ± 0.09 | 1.25 ± 0.11 | 1.24 ± 0.07 |

Table 1: Table of statistical estimators for NNPDF2.1 with $N_{\text{rep}} = 1000$ replicas (first columns). The subsequent columns show the corresponding results, to be discussed in Sect. 4, for fits to central data and with fixed partitions, with $N_{\text{rep}} = 100$ replicas each. All entries in the last column are obtained repeating the procedure for five random choices of fixed partition and averaging the final results. All values are normalized to the number of data points.

More detailed tests can be performed by looking at the distance between estimators extracted from PDF sets, defined as follows. Given a set of $N_{\text{rep}}^{(i)}$ PDF replicas, the estimator for any quantity q computed from the PDFs (including the PDFs themselves) is the mean $\langle q \rangle_{(i)} = \frac{1}{N_{\text{rep}}^{(i)}} \sum_{k=1}^{N_{\text{rep}}^{(i)}} q_k$. The distance between two determinations of q from sets $q_i^{(1)}, q_i^{(2)}$ is then

$$d^2 \left(\langle q^{(1)} \rangle, \langle q^{(2)} \rangle \right) = \frac{(\langle q^{(1)} \rangle_{(1)} - \langle q^{(2)} \rangle_{(2)})^2}{\sigma_{(1)}^2[\langle q^{(1)} \rangle] + \sigma_{(2)}^2[\langle q^{(2)} \rangle]}, \quad (1)$$

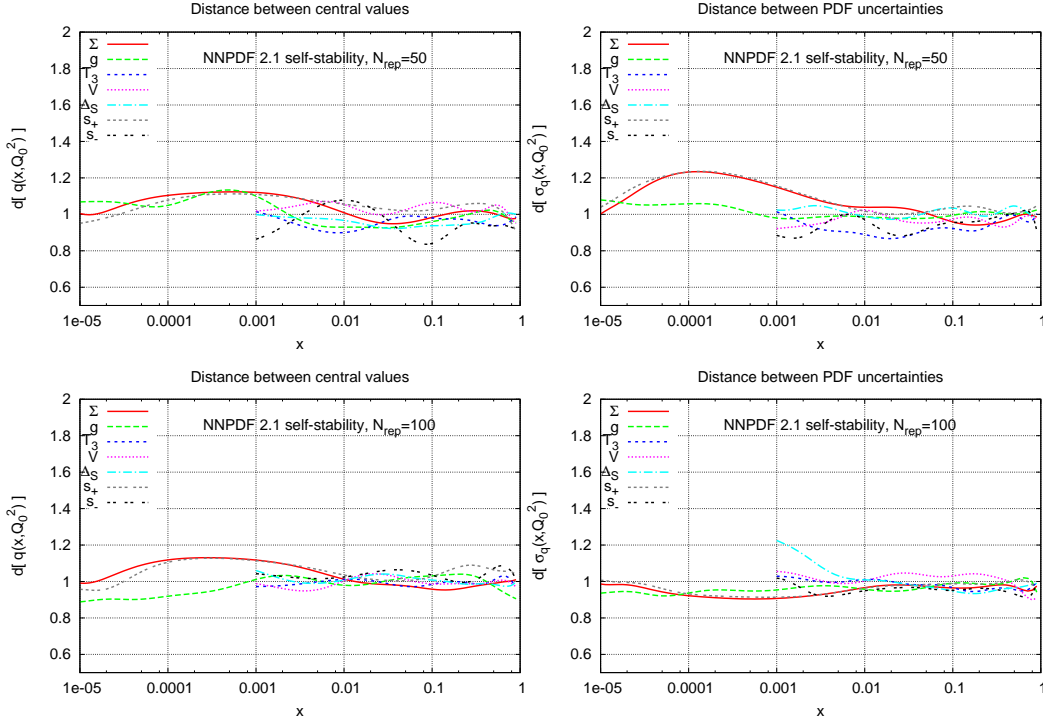


Fig. 1: Distances between central values and uncertainties of PDFs computed from two distinct sets of $N_{\text{rep}} = 50$ (top) or $N_{\text{rep}} = 100$ replicas (bottom).

with the variance of the mean given by

$$\sigma_{(i)}^2[\langle q^{(i)} \rangle] = \frac{1}{N_{\text{rep}}^{(i)}} \sigma_{(i)}^2[q^{(i)}] \quad (2)$$

in terms of the variances $\sigma_{(i)}^2[q^{(i)}]$ of the variables $q^{(i)}$ (which a priori could come from two distinct probability distributions). The distance between uncertainties can be defined in a similar way. By construction, the probability distribution for the distance coincides with the χ^2 distribution with one degree of freedom, and thus it has mean $\langle d \rangle = 1$, and $d \lesssim 2.3$ at 90% confidence level.

An immediate use of the distance is to check that PDF sets computed from different sets of replicas are statistically equivalent (i.e. that $\langle q^{(k)} \rangle_{(i)}$ has the expected distribution). This is shown in Fig. 1 (top row): indeed distances fluctuate about $d \sim 1$. Furthermore, one can check (Fig. 1, bottom row) that the distance does not change as the number of replicas is varied: because of the explicit factor of $\frac{1}{N_{\text{rep}}^{(i)}}$ in

Eq. (2), this verifies that indeed the uncertainty of the mean decreases as $1/\sqrt{N_{\text{rep}}^{(i)}}$ as $N_{\text{rep}}^{(i)}$ is increased. Note that this means that the distance between two PDFs that barely overlap within error bands at 68% C.L. with $N_{\text{rep}} = 100$ replicas is $\langle d \rangle \sim 7$ (because the distance is computed averaging results from subsets of $N_{\text{rep}}/2 = 50$ replicas [7]).

Next, we check the independence of results of the parametrization. This is done by constructing a new set of PDF replicas with a different choice of architecture for neural networks, and checking that results are statistically equivalent. In Fig. 2 we show the distances between PDFs based on the default architecture 2–5–3–1. and PDFs based on the smaller 2–4–3–1 architecture. This corresponds to removing 6 free parameters from the parametrization of each PDF, i.e. removing of 42 free parameters overall. The similarity of Figs. 1 and 2 proves the stability of results. Note that, in order to make sure that the parametrization is indeed redundant, the larger architecture is used as a default.

Finally, we turn to our most detailed test of the statistical consistency of PDFs determined with

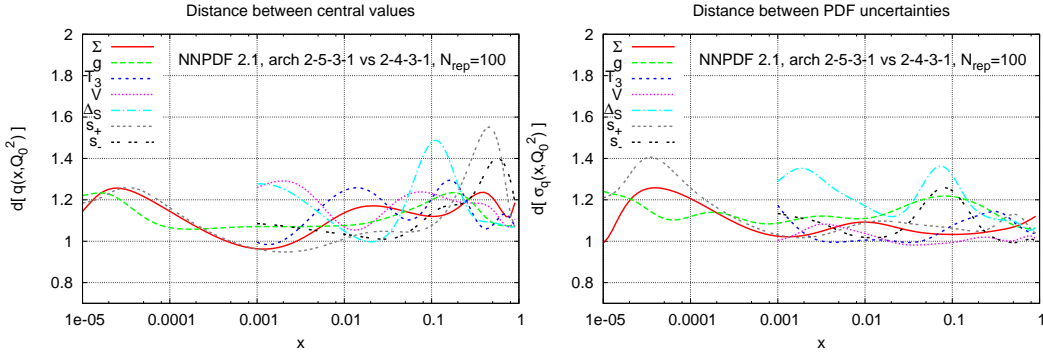


Fig. 2: Distances between PDFs with the default neural network architecture (2–5–3–1) and a reduced architecture (2–4–3–1).

the NNPDF methodology. Namely, we exploit the fact that given the probability distribution $\mathcal{P}_{\text{old}}(f)$ for PDFs determined from a certain starting dataset, the effect of the inclusion of the information from new data can be determined using Bayes’ theorem. It is then possible to compare the probability distribution $\mathcal{P}_{\text{new}}(f)$ obtained in this way, with a determination of $\mathcal{P}_{\text{new}}(f)$ found by simply performing a fit to an extended dataset including both the starting dataset and the new data. Statistical equivalence of the two determinations of $\mathcal{P}_{\text{new}}(f)$ shows that the NNPDF methodology treats the information contained in the data in a consistent way. In fact, repeating this test for all of the data used for the fit, to the extent that for a large enough dataset results are independent of the prior assumption, would amount to a proof that the set of data and the set of PDFs determined from it contain the same information (“closure test”): indeed, such a Bayesian procedure was suggested in Ref. [11] as a way of arriving at a fully unbiased and self-consistent PDF determination.

We have performed such a test for an individual subset of data included in the NNPDF2.1 NLO PDF determination. The formalism to do so was developed in Ref. [12, 13], correcting a previous proposal of Ref. [14]. The way it works is the following: assume we want to include n new data $y = \{y_1, y_2, \dots, y_n\}$ which had not been originally included in the determination of the initial probability density distribution. We view this data as a point y in an n -dimensional space, with uncertainties given as a $n \times n$ experimental covariance matrix. We update the probability density $\mathcal{P}_{\text{old}}(f)$ using the conditional probability of the new data, which is proportional to the probability density of the χ^2 to the new data conditional on f :

$$\mathcal{P}(\chi^2|f) \propto (\chi^2(y, f))^{\frac{1}{2}(n-1)} e^{-\frac{1}{2}\chi^2(y, f)}, \quad (3)$$

where $y_i[f]$ is the value predicted for the data y_i using the PDF f . By Bayes’ theorem then

$$\mathcal{P}_{\text{new}}(f) = \mathcal{N}_\chi \mathcal{P}(\chi|f) \mathcal{P}_{\text{old}}(f), \quad (4)$$

(with \mathcal{N}_χ an f -independent normalization factor).

Using Eq. (3) in Eq. (4) immediately implies that the inclusion of the new data can be viewed as a reweighting of the prior probability distribution $\mathcal{P}_{\text{old}}(f)$. Namely, if the expectation value of some observable \mathcal{O} with the distribution $\mathcal{P}_{\text{old}}(f)$ is

$$\langle \mathcal{O} \rangle = \frac{1}{N} \sum_{k=1}^N \mathcal{O}[f_k], \quad (5)$$

then, by Eq. (4), its expectation value according to $\mathcal{P}_{\text{old}}(f)$ is

$$\langle \mathcal{O} \rangle_{\text{new}} = \frac{1}{N} \sum_{k=1}^N \mathcal{N}_\chi \mathcal{P}(\chi|f_k) \mathcal{O}[f_k] = \frac{1}{N} \sum_{k=1}^N w_k \mathcal{O}[f_k], \quad (6)$$

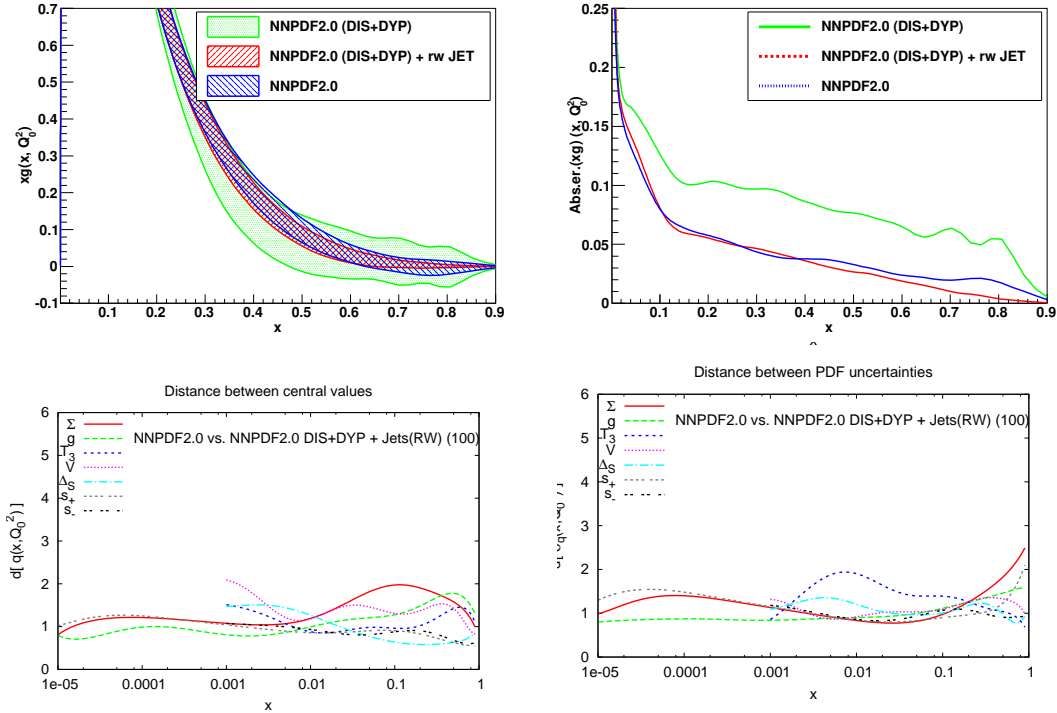


Fig. 3: Top: the gluon distribution (left) and its uncertainty (right) of the NNPDF2.0(DIS+DY) fit before and after reweighting with the inclusive jet data compared to the refitted gluon from NNPDF2.0. Bottom: distances between the refitted and reweighted results for central values (left) and uncertainties (right).

with

$$w_k = \frac{(\chi_k^2)^{\frac{1}{2}(n-1)} e^{-\frac{1}{2}\chi_k^2}}{\frac{1}{N} \sum_{k=1}^N (\chi_k^2)^{n/2-1} e^{-\frac{1}{2}\chi_k^2}}. \quad (7)$$

The weights w_k , when divided by $N = N_{\text{rep}}$, are just the probabilities of the replicas f_k , given the χ^2 to the new data.

The comparison between the “reweighted” result Eq. (6-7) and the refitted one is shown in Fig. 3: it is apparent that the two procedures lead to the same result, except possibly at very large $x \gtrsim 0.7$ where the determination becomes unreliable because of the lack of experimental information. This is a very strong check that PDF uncertainties admit a *bona fide* statistical interpretation, and thus should not be viewed of theoretical uncertainties with unknown distribution. Note that because NNPDF results are delivered as a Monte Carlo sample, any feature of the distribution of results, such as confidence intervals or higher moments, can be determined explicitly.

3 Dataset dependence

One important feature of the NNPDF approach is that the same methodology can be used to determine PDFs from datasets of rather different size and nature: this, in particular, follows from the extreme redundancy of the parametrization, and the ensuing parametrization independence, explicitly checked in the previous section. In fact, NNPDF results are even stable upon the addition of new independently parametrized PDF, as seen in Ref. [5, 6] where light quark and gluon PDFs were found to be stable upon addition of an independent parametrization of strangeness. This is to be contrasted to the approach used by other groups, where a larger dataset requires the introduction of more parametr. As a consequence, in the NNPDF approach, unlike in other approaches, the addition of new compatible data results in error reduction, as has been checked explicitly in benchmark studies [5, 15].

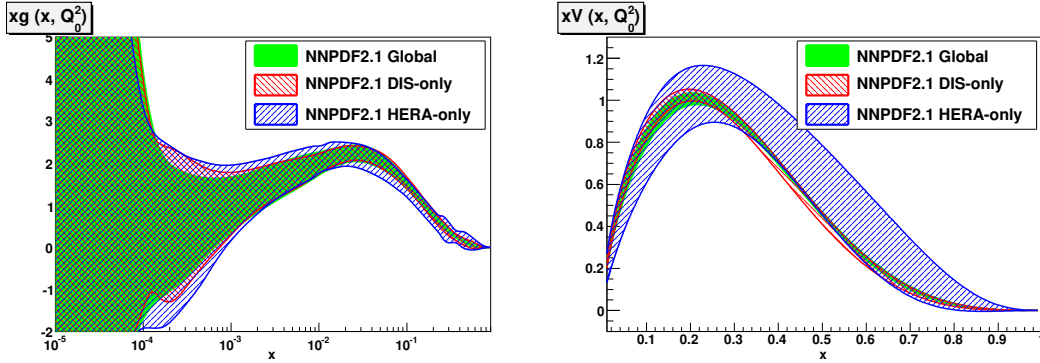


Fig. 4: Comparison of PDFs obtained to fits to different datasets: a global fit, a DIS-only fit and a HERA-only fit. The gluon (left) and total valence (right) PDFs are shown.

By comparing the results of fits to different datasets it is then possible to study the effect of individual data on PDFs and verify their consistency. For example, in Fig. 4, we compare the default NNPDF2.1 PDF set to PDFs obtained using only the DIS data or only the HERA DIS data from the global dataset. On the one hand, it is apparent from this comparison that these fits are mutually consistent; on the other hand it is clear that the HERA data determine well the small x gluon, the DIS data also determine well the total valence (mostly due to neutrino data), while the global dataset further improves the large x gluon. Detailed studies of this kind are performed in Refs. [8, 9] (see Ref. [1] for a general discussion of the expected impact of different data on PDFs).

A more detailed consistency check is performed by comparing fits in which a certain "new" dataset is added to different pre-existing datasets, and verifying that the impact of new data is independent of the choice of the dataset to which they are added, thereby also verifying the mutual consistency of the various data subsets involved. One such comparison (within the framework of the NNPDF2.0 [8] PDF set) is shown in Fig. 5 in which the effect of Drell-Yan data on the total valence and strange valence PDFs are compared when these data are added to a fit to DIS data only, or to a fit to DIS+jet data. More tests of this kind were shown in Ref. [1] and demonstrated equally good consistency.

The consistency of different data can be addressed quantitatively using the Bayesian reweighting technique of Ref. [12] summarized in Sect. 2. Namely, assume that the covariance matrix for a given dataset is rescaled by a common factor α , $\sigma_{ij} \rightarrow \alpha \sigma_{ij}$ so that for that experiment $\chi^2 \rightarrow \chi^2/\alpha^2$. It is then easy to show [12] that the probability density $\mathcal{P}(\alpha)$ for α given the data is

$$\mathcal{P}(\alpha) \propto \frac{1}{\alpha} \sum_{k=1}^N w_k(\alpha), \quad (8)$$

where $w_k(\alpha)$ are the weights Eq. (7) evaluated with the rescaled covariances. If $\mathcal{P}(\alpha)$ peaks close to one the new data are consistent, while if it peaks far above one, then it is likely that the errors in the data have been underestimated. As an example, we show in Fig. 6 $\mathcal{P}(\alpha)$ computed for two of the Tevatron D0 lepton asymmetry datasets analyzed in [12]. For muon data [16] $\mathcal{P}(\alpha)$ is peaked close to one, implying that this dataset is consistent with the other sets in the global fit. For muon data $\mathcal{P}(\alpha)$ is peaked far from one, suggesting that experimental uncertainties have been underestimated by about a factor two.

4 Functional and Data components of the PDF uncertainty

Because PDFs are functions determined from a finite set of data, one may expect that on top of the propagated uncertainty due to the uncertainty in the data there might be a further uncertainty due to existence (for sufficiently general parametrization) of many PDFs which give a fit of the same quality to the data.

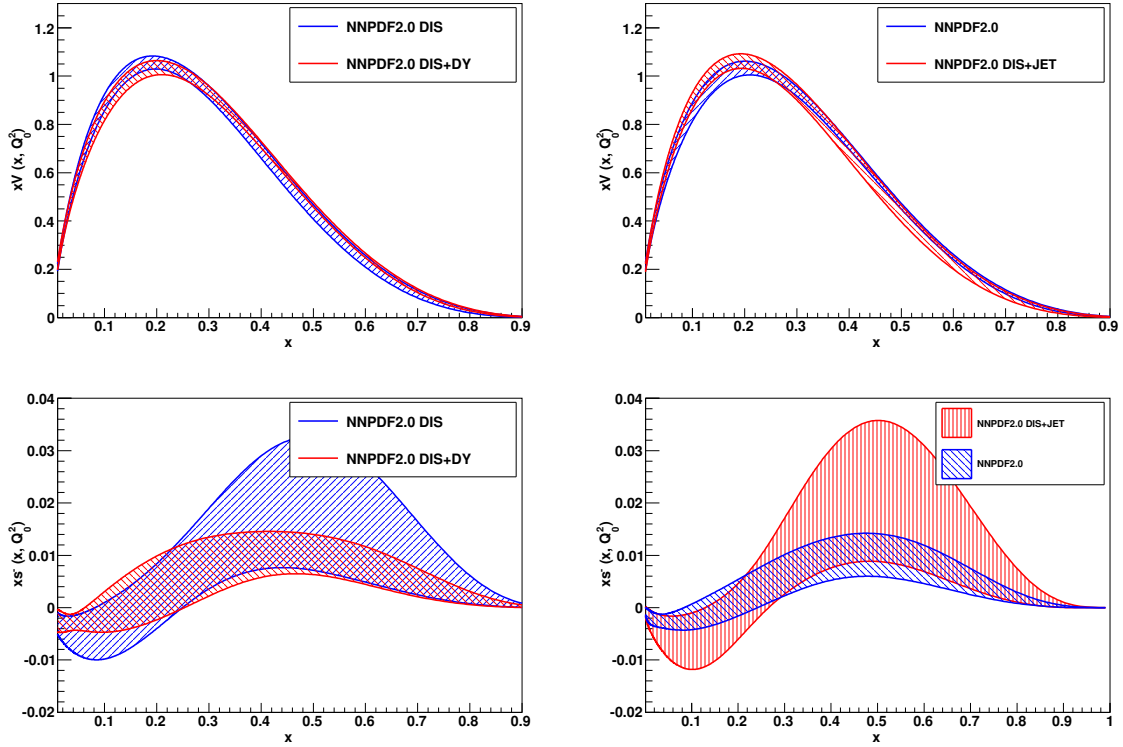


Fig. 5: Impact of the inclusion of Drell–Yan data in a fit with DIS data only (left), and in a fit with DIS and jet data (right). From top to bottom, total valence and $s - \bar{s}$ PDFs.

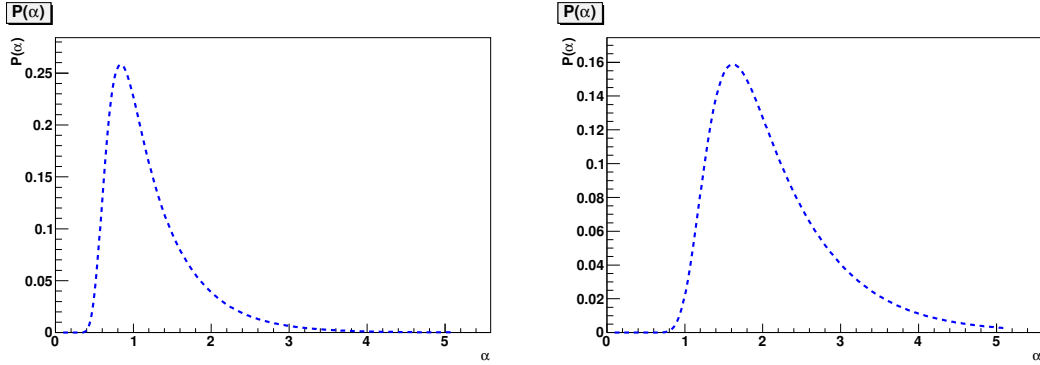


Fig. 6: The probability distribution $\mathcal{P}(\alpha)$ for the D0 lepton asymmetry data uncertainty to be underestimated by a factor α : muon data [16] (left) and electron data [17] (right).

For definiteness, we will call these different sources of uncertainty “data” and “functional” uncertainty respectively. If one were to accept infinitely coarse (e.g. fractal) PDF shapes the functional uncertainty would be infinite, but even if it is kept under control by some smoothness assumption it will generally still be nonzero. In fact, it was recently argued in Ref. [18] that the so called “tolerance” criterion [19] in PDF fits which make use of underlying functional forms with a relatively small number of parameters, and amounts to a rescaling of the $\Delta\chi^2$ range used to determine the one- σ range, mostly accounts for the fact that the choice of a fixed functional form with few parameters substantially underestimates the functional uncertainty.

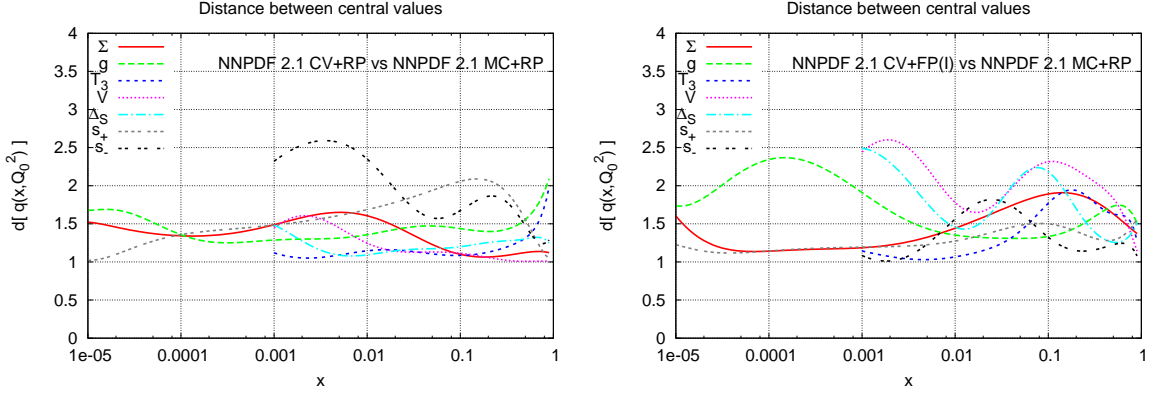


Fig. 7: Distances between central values of the reference PDFs and those fitted to different partitions of central values (left) or to a fixed partition of central values (right).

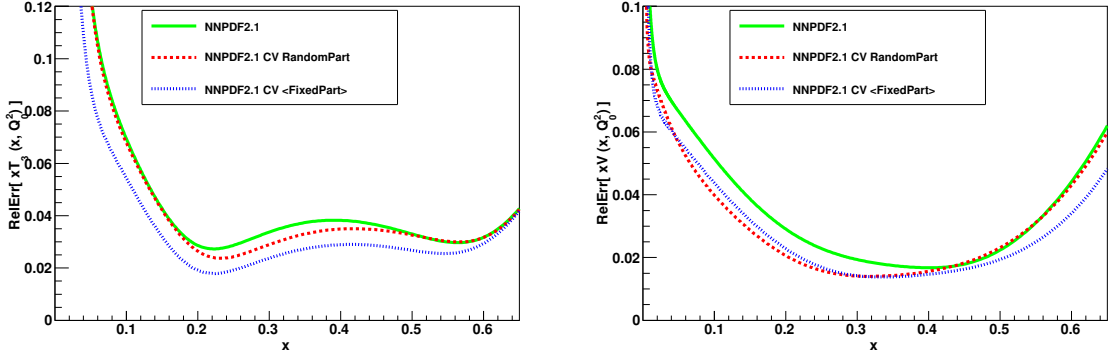


Fig. 8: Comparison between relative PDF uncertainties of the reference PDF set, a fit to varying partitions of central values and a fit to a fixed partition of central values for the isotriplet $T_3(x)$ (left) and the total valence $V(x)$ (right).

In the NNPDF approach, we can actually estimate the relative size of the data and functional uncertainty by constructing PDF replica sets based on a frozen set of data, as we now discuss. First, we switch off the pseudodata generation. Each PDF replica is then fitted to the same central data values (CV fit). However, each replica is still fitted to a different subset of data because for each replica the data are randomly divided in a training and validation set. Next, we also switch off the random partitioning of data for each replica, and we simply fit all PDF replicas to the same partition of central values (FP). In the latter case, the procedure is repeated five times, with different choices of the fixed partition in each case, in order to make sure that there is nothing special about the single partition that has been chosen in the first place, and results are the averaged.

Results for the statistical estimators for these fits are compared to those of the default case in Table 1. Furthermore, in Fig. 7 we display the distances between central values of PDFs obtained in the various cases, while in Fig. 8 we compare the relative percentage uncertainties for a couple representative PDFs. The central values appear to be very stable (distances of order one) and indeed the fit quality as measured by χ_{tot}^2 is essentially the same in all cases. When the pseudodata generation is switched off, $\langle E \rangle$, the average quality of the fit of each replica to the corresponding data replica now by construction coincides with $\langle \chi^{2(k)} \rangle$ (the same quantity but computed for central data). Interestingly, the value of $\langle \chi^{2(k)} \rangle$ in the reference and CV fit is identical: this confirms that the fitting methodology is very efficient in removing the extra fluctuation of the pseudodata about their central values induced by the pseudodata

| Dataset | σ Data (%) | σ Ref. (%) | σ CV (%) | σ FP (%) |
|----------|-------------------|-------------------|-----------------|-----------------|
| TOTAL | 11.3 | 3.7 | 3.8 | 3.1 ± 0.2 |
| NMC-pd | 1.9 | 0.5 | 0.5 | 0.4 ± 0.03 |
| NMC | 5.0 | 1.6 | 1.6 | 1.4 ± 0.2 |
| SLAC | 4.4 | 1.7 | 1.7 | 1.4 ± 0.3 |
| BCDMS | 5.7 | 2.6 | 2.8 | 2.3 ± 0.3 |
| HERAI-AV | 2.5 | 1.3 | 1.3 | 1.1 ± 0.1 |
| CHORUS | 15.1 | 4.5 | 5.3 | 3.4 ± 0.3 |
| FLH108 | 72.0 | 4.1 | 3.9 | 3.9 ± 0.5 |
| NTVDMN | 21.1 | 14.5 | 14.1 | 12.7 ± 1.6 |
| ZEUS-H2 | 13.4 | 1.3 | 1.3 | 1.1 ± 0.2 |
| ZEUSF2C | 23.3 | 3.1 | 3.1 | 2.8 ± 0.2 |
| H1F2C | 17.3 | 2.9 | 2.9 | 2.6 ± 0.2 |
| DYE605 | 22.3 | 8.1 | 7.0 | 6.1 ± 0.3 |
| DYE886 | 20.1 | 9.1 | 8.3 | 8.2 ± 0.4 |
| CDFWASY | 6.0 | 4.5 | 3.4 | 3.1 ± 0.3 |
| CDFZRAP | 11.5 | 3.5 | 3.6 | 3.5 ± 0.5 |
| D0ZRAP | 10.2 | 2.8 | 3.0 | 2.9 ± 0.5 |
| CDFR2KT | 22.8 | 4.8 | 4.4 | 4.4 ± 0.2 |
| D0R2CON | 16.8 | 5.5 | 5.1 | 5.1 ± 0.2 |

Table 2: The average percentage uncertainty for each datasets for the reference, central value, and fixed partition PDF sets.

generation. It also suggests that the pseudodata generation is barely necessary. In fact, one could take this CV fit as a default: the fluctuations in central data are then just reproduced by bootstrap, by the process of choosing different partitions. Indeed, comparison of PDF uncertainties in the reference and CV case shows that they are very close and only moderately larger in the reference case, so that even if the pseudodata generation is viewed as a more conservative way of estimating uncertainties, in practice it is seen to have little effect.

However, the most striking result is given by the PDF uncertainties in the FP case: these uncertainties, though somewhat smaller, are still of the same order of magnitude as those of the the standard fit. This means that different replicas constructed by refitting exactly the same data over and over again still have a non-negligible spread and thus uncertainty. This is only possible because of the random nature of the fitting algorithm, and it shows that indeed there is a nontrivial space of almost equivalent minima. It should be noticed that indeed the fluctuation of $\langle \chi^2(k) \rangle$ for this replica set is significantly smaller than for the reference and CV sets, consistent with the hypothesis that one is now exploring a space of equivalent or almost equivalent minima.

A more quantitative insight on the relative size of various contributions to the uncertainties can be obtained by computing the average uncertainty on the prediction for the fitted observables obtained using each PDF set. These are shown, both for the global and individual dataset, in Table 4, where the starting data uncertainty is also shown for comparison. The uncertainties obtained fitting to central data or to pseudodata replicas are almost identical: as already noticed, one might as well fit to central data. Both are significantly smaller than the original data uncertainty, thereby showing that an underlying law has been learnt. The residual uncertainty in the FP case is still sizable. If one assumes that the uncertainty in the FP case is the functional uncertainty, while in the CV case it is the sum in quadrature of data and functional uncertainty, then one concludes that the functional uncertainty is rather more than half the total uncertainty.

5 Outlook

Having verified that PDFs determined with the NNPDF methodology are consistent with statistical expectations and free of parametrization bias, it is natural to think that some of the statistical tools discussed here, as well as more refined statistical tests, may be used to guide and validate further improvements.

Two aspects of the methodology may be amenable to improvement. The first has to do with the underlying functional form. At present, PDFs are parametrized as a neural network, multiplied by a preprocessing function of the form $x^\alpha(1-x)^\beta$. The exponents are then randomly varied in a reasonable range. The preprocessing speeds up the fitting of the neural network, and ensures that outside the data region the behaviour of the PDF does not fluctuate too wildly. This procedure is much more general and unbiased than that used in fits such as MSTW or CTEQ, in which the functional form also incorporates the same small- and large- x behaviour, but the exponents α and β are fitted (instead of being varied in a range around their best fit) and the residual number of parameters is smaller by more than one order of magnitude. But the preprocessing could still be a source of residual bias, so one should check whether results are stable upon completely different choices of preprocessing. The second has to do with the determination of the best fit. While cross-validation is quite efficient on average, it could still lead to some specific dataset being under- or overlearned; it involves some arbitrariness, for instance in deciding the precise form of the stopping criteria; and it could lead to an excessively wide and thus sub-optimal space of minima. Hence alternative methods to determine the optimal fit should be explored.

Correspondingly, two sets of statistical investigations may be worth pursuing in order to guide and validate these improvements. On the one hand, it may be interesting to study the form of the probability distributions of PDF replicas: for instance, this could allow one to directly address the question of what in a conventional procedure is the $\Delta\chi^2$ range which corresponds to a 68% confidence interval. On the other hand, it may be useful to investigate systematically the statistical impact of each dataset, with the aim of arriving at a full “closure test” — a proof that there is no information loss in extracting PDFs from data. These improvements may be useful and even necessary for precision phenomenology at the LHC.

Acknowledgments: We thank G. Cowan, L. Lyons and H. Prosper for discussions and encouragement. M.U. is supported by the Bundesministerium für Bildung and Forschung (BmBF) of the Federal Republic of Germany (project code 05H09PAE). This work was partly supported by the Spanish MEC FIS2007-60350 grant.

References

- [1] S. Forte, *Acta Phys.Polon.* **B41** (2010) 2859–2920, [1011.5247].
- [2] S. Forte, L. Garrido, J. I. Latorre, and A. Piccione, *JHEP* **05** (2002) 062, [hep-ph/0204232].
- [3] L. Del Debbio, S. Forte, J. I. Latorre, A. Piccione, and J. Rojo, **The NNPDF Collaboration** *JHEP* **03** (2005) 080, [hep-ph/0501067].
- [4] L. Del Debbio, S. Forte, J. I. Latorre, A. Piccione, and J. Rojo, **The NNPDF Collaboration** *JHEP* **03** (2007) 039, [hep-ph/0701127].
- [5] R. D. Ball *et. al.*, **The NNPDF Collaboration** *Nucl. Phys.* **B809** (2009) 1–63, [0808.1231].
- [6] J. Rojo *et. al.*, **The NNPDF Collaboration** 0811.2288.
- [7] R. D. Ball *et. al.*, **The NNPDF Collaboration** *Nucl. Phys.* **B823** (2009) 195–233, [0906.1958].
- [8] R. D. Ball *et. al.*, **The NNPDF Collaboration** *Nucl. Phys.* **B838** (2010) 136–206, [1002.4407].
- [9] R. D. Ball, V. Bertone, F. Cerutti, L. Del Debbio, S. Forte, *et. al.*, *Nucl.Phys.* **B849** (2011) 296–363, [1101.1300].
- [10] R. D. Ball *et. al.*, **The NNPDF Collaboration** *JHEP* **05** (2010) 075, [0912.2276].
- [11] W. T. Giele, S. A. Keller, and D. A. Kosower, hep-ph/0104052.
- [12] R. D. Ball *et. al.*, **The NNPDF Collaboration** *Nucl.Phys.* **B849** (2011) 112–143, [1012.0836].

- [13] R. D. Ball, V. Bertone, F. Cerutti, L. Del Debbio, S. Forte, *et. al.*, **The NNPDF Collaboration** 1108.1758.
- [14] W. T. Giele and S. Keller, *Phys. Rev.* **D58** (1998) 094023, [hep-ph/9803393].
- [15] M. Dittmar *et. al.*, 0901.2504.
- [16] V. M. Abazov *et. al.*, **D0 Collaboration** *Phys. Rev.* **D77** (2008) 011106, [0709.4254].
- [17] V. M. Abazov *et. al.*, **D0 Collaboration** *Phys. Rev. Lett.* **101** (2008) 211801, [0807.3367].
- [18] J. Pumplin, *Phys. Rev.* **D82** (2010) 114020, [0909.5176].
- [19] J. Pumplin *et. al.*, *JHEP* **07** (2002) 012, [hep-ph/0201195].